BRDF LABORATORY MEASUREMENTS USING A CAMERA-AIDED SPECTRORADIOMETER

Elena Roitberg, Itamar Malgeac, Shachaf Weil-Zattelman, and Fadi Kizel*

Dept. of Mapping and Geoinformation Engineering, Technion-Israel Institute of Technology, Haifa, 32000.
elenaroi@technion.ac.il; itamarm@campus.technion.ac.il; shaweil@campus.technion.ac.il;fadikizel@technion.ac.il

KEY WORDS: Remote sensing, Spectral measurements, BRDF, Spectroradiometer, Structure from Motion (SFM).

ABSTRACT:

Numerous natural surfaces observed using Remote Sensing do not reflect light as Lambertian surfaces. Instead, their reflection is highly dependent on two main directions: the direction of the light source and the observation viewing angle, which characterize the Bidirectional Reflectance Distribution Function (BRDF). The BRDF is one of the challenging main effects of remote sensing. Thus, studying the BRDF of various land cover surfaces is essential, and researchers invest many efforts to fulfill this objective. However, measuring the BRDF is tricky and requires unique instruments, e.g., the Gonioreflectometer. Unfortunately, the availability of such instruments is deficient, and they are costly and hard to maintain. Considering these limitations, we present a study and a new approach for measuring the BRDF of surfaces with a camera-aided spectroradiometer that simultaneously acquires an RGB image from the sensor location beside the spectral measurement. Then, we feed the Structure From Motion (SFM) process with the RGM images to retrieve the sensor locations. Next, we convert the sensor locations into the quantities needed for the BRDF measurement, i.e., zenith angles and distances relative to the measured sample. Finally, we apply a set of measurements under controlled conditions in a dark room designed for hyperspectral remote sensing studies to evaluate the proposed methodology. In particular, we experimented with three different material surfaces. The results clearly show the highly accurate sensor position derived by SFM, providing zenith angles and distance from the scene's center with mean errors around one degree and 2.5 centimeters, respectively. In addition, the obtained spectra tell that the proposed approach is suitable for multiangular measurements of reflected light and studying the BRDF.

1. INTRODUCTION

1.1 BRDF of non-Lambertian surfaces and conventional instruments for its' measuring

The Bidirectional Reflectance Distribution Function (BRDF) (Nicodemus et al., 1977) is one of the challenging main effects in remote sensing. The BRDF represents how light is reflected from a surface in different directions. Usually, we define the BRDF by four variables (Silva, 1978) as follows:

$$f_r(\theta_i,\phi_i;\theta_r,\phi_r)=\frac{dL_r(\theta_i,\phi_i;\theta_r,\phi_r)}{dE_i(\theta_i,\phi_i)}\left[sr^{-1}\right], \quad (1)$$

where $dL_r\left[W\cdot m^{-2}\cdot sr^{-1}\right]$ and $dE_i\left[W\cdot m^{-2}\right]$ denote the outgoing radiance from the surface in direction θ_r,ϕ_r and the incoming irradiance from the direction θ_i,ϕ_i, respectively.

Understanding the BRDF of landcover types is essential and relies mainly on measuring the multiangular surface reflectance and analyzing their variability (Martonchik et al., 2000). Such measurements usually require unique and expensive instruments (e.g., Gonioreflectometer (White et al., 1998; Li et al., 2006)) that allow for accurate placement of the measuring device (i.e., the spectroradiometer) and the light source. A Gonioreflectometer allows for estimating the surface's BRDF by measuring the reflected light across the hemisphere. The hemisphere radius is a fixed feature of the device. The placement of the light source and the radiance measuring device vary upon a hemisphere, while the target is placed in the hemisphere center. A Gonioreflectometer is usually built particularly per project (Lanevski et al., 2022), and any changes in target dimensions will necessitate purchasing a new system.

Unfortunately, the availability of a Gonioreflectometer within remote sensing laboratories is not very high due to its high cost, the space required for it, and its challenging maintenance. On the other hand, the availability of RGB cameras hugely increased in the recent two decades, and they have become smaller and effortless to handle (through smartphones, for example). Besides, several spectroradiometers are now aided with an RGB camera that allows for simultaneously imaging the measured area, e.g., the Spectral Evolution RS-8800.

RGB images acquired from the exact location as the spectroradiometer's probe tip enable an automatic derivation of the measurement direction without using special instruments. Specifically, using the computer vision algorithm, Structure from Motion (SFM) (Onur¨ et al., 2017), we can automatically derive each image's camera position and retrieve the spectroradiometer's location in each measurement.

This work proposes a new technique for measuring the BRDF using a spectroradiometer combined with an RGB camera, i.e., camera-aided.

1.2 A novel approach for BRDF measurements

The camera-aided approach replaces the usually used metal arcs-based rigid device called Gonioreflectometer. In contrast to Gonioreflectometer, the camera-aided spectrometer is not

- Corresponding author.

limited to the specified distance between the spectrometer probe and the object, the restriction dictated by the rigid construction of the goniometer, which prescribes the FOV of the spectrometer and sometimes may too large or too small and appropriate for the observed target. Moreover, the suggested method implies a simple RGB camera which is incomparably cheaper than a massive Gonioreflectometer.

1.2.1 Structure From Motion (SFM) for sensor positioning

Given a set of images of the same scene but from different directions and locations, the SFM (Özyeşil et al., 2017) technique reconstructs the scene's 3D structure model. Besides, a valuable output of the method is the 3D camera position for each image. The main steps of the SFM include 1) feature extraction from each image, 2) feature matching for image pairing and connectivity mapping, 3) triangulation and bundle adjustment for camera positioning, and 4) model extraction. Both outputs of the SFM, i.e., the 3D model and camera positions, are helpful for BRDF measurements.

We use the advantage of camera-aided spectrometers and acquire an RGB image corresponding to each spectral measurement. Then, we feed the SFM with these images to estimate the sensor locations. Then, we convert these locations into angular directions essential for BRDF measurements (i.e., the zenith angle corresponding to each spectral measurement (see Figure 5).

2. METHODOLOGY

The inclination angle of the spectroradiometer probe and its' location relative to the target and the light source position are necessary for BRDF calculations. Therefore, we conduct an experiment with two stages to test the capabilities of the camera-aided spectroradiometer to retrieve the geometrical parameters required for BRDF measurements.

In the first stage, we built an auxiliary device that allows measuring the target's reflectance from different directions and a fixed distance (see details in 3.2). This controlled arrangement allows for the development of the second stage, which will implement the proposed method for BRDF measurements with camera aided spectroradiometer without any auxiliary devices. Besides, we use the zenith angle and distance obtained from the auxiliary device as ground truth (GT) to validate the estimated zenith angles and distances retrieved using the proposed SFM-based approach.

2.1 BRDF measurements

The BRDF is, in practice, theoretical since measuring the incident and reflected light in particular directions is not possible. Thus, in remote sensing, we instead estimate the BRDF by measuring the Biconocal Reflectance Factor (BCRF). Measuring the BCRF at various observation angles includes a ratio of radiance reflected from the observed material in the observed direction and the incident irradiance. One way to obtain the incident irradiance relies on measuring the radiance reflected from a reference Lambertian surface of Barium-sulfate. In our case, we measure the Lambertian surface from the nadir direction. Besides, the light source remains constant during the experimental set; therefore, we assume that its irradiance did not change significantly during the measurements. Finally, in the rest of the work, we refer to the BRDF term, but as accepted in remote sensing applications, we measure the BCRF.

2.2 Estimating the sensor's zenith angle from the SFM outputs

The scene's 3D model and camera locations obtained using the SFM are in an arbitrary coordinate system. However, for BRDF measurement, we need to estimate the angular location of the sensor in each image relative to the scene's normal. In our case, the normal's direction is the same as the direction from the scene's center to the vertical image, i.e., the image with a zenith angle equal to zero. Thus, we compute the zenith angle for each image (i.e., sensor's location) relative to this direction as follows: Let $\mathbf{p}_t \in \mathbb{R}^{3\times1}$ denote a point in an arbitrary coordinate system with three ordinates x, y, z, i.e., $\mathbf{p}_t = \left[x_t, y_t, z_t\right]^T$, and let $\mathbf{p}_0$ be the point representing the scene's center; we define the vector from $\mathbf{p}_0$ to $\mathbf{p}_t$ as:

$$\mathbf{u}_t = \mathbf{p}_t - \mathbf{p}_0, \tag{2}$$

and the distance from $\mathbf{p}_0$ to $\mathbf{p}_t$ as:

$$d_t = \left\|\mathbf{u}_t\right\|. \tag{3}$$

Accordingly, we define $\mathbf{u}_v$, and $\mathbf{u}_j$ as the two vectors from $\mathbf{p}_0$ to the points representing the camera position of the vertical and the *jth* image, respectively.
Then, we calculate the zenith angle of the *jth* image as follows:

$$\theta_i^j = \arccos\left(\frac{\mathbf{u}_v^T\mathbf{u}_j}{\left\|\mathbf{u}_v\right\|\cdot\left\|\mathbf{u}_j\right\|}\right). \tag{4}$$

The distance between the RGB camera and the spectral sensor in our setup is neglectable in terms of the zenith angle and distance from the scene's center. Thus, we assume that the spectral sensor locations in the BRDF scene are similar to those of the RGB images.

3. EXPERIMENTAL SETUP AND MATERIALS

We implement an experimental setup with the following main components: a spectroradiometer, light source, and RGB camera. The specifications of the spectroradiometer are presented in detail in 3.1. A halogen bulb was used as a light source since it simulates a sunlight spectrum and allows radiance measurements from 350 to 2500 nm. Then, we examined two configurations of camera-aided spectrometers, 1) with a built-in RGB camera and 2) with an RGB camera of a cellular phone that we connected to the spectroradiometer fiber optic probe and used for the observed scene imaging. However, due to space limitations, we present the results of only the second configuration. We will address the results of the two configurations and their comparison in our future work.

3.1 Spectroradiometer specifications

We used the Field Portable Spectroradiometer of Spectra Vista Corporation GER2600 with a fiber optic probe, which provides high-resolution irradiance measurements. We attached a smartphone to the GER2600 to simultaneously acquire an RGB image of the measured area. The spectroradiometer has 640 spectral bands ranging from 350 to 2500nm. The FOV of the fiber optic probe is 25deg. The spectral resolution is as follows: 1.5 nm /3.2 nm at 350 nm to 1050 nm and 11.5 nm/ 30 nm at 1050nm to 2500 nm.

3.2 Experimental setup

The BRDF camera aided-spectroradiometer experiments were carried out in a dark room with no diffused light from outside. A

halogen light source that simulates solar radiation was used as the only light source.

The auxiliary device is built of a rotating arm around a pivot connected to a table where the target materials were placed. The measurements of the sensor's locations from the auxiliary device served to evaluate the retrieved location by SFM and ensure that the distance between the spectroradiometer probe and the target remained constant.

A protractor was mounted adjacent to the table to determine the sensor's zenith angle. These setup configurations enabled measurements from -90 to 90 degrees along the principal plane (Figure 1). The zenith angle of the light source was about 33 degrees (Figure 2).

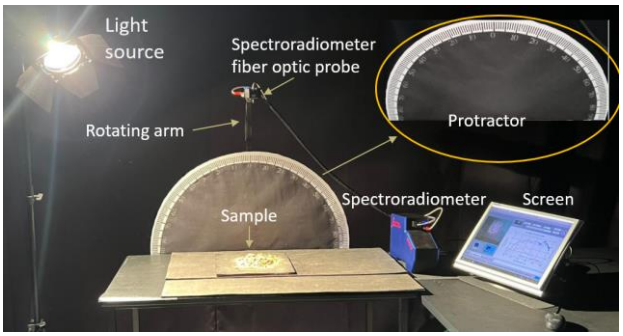

Figure 1. Experimental setup for BRDF measurments.

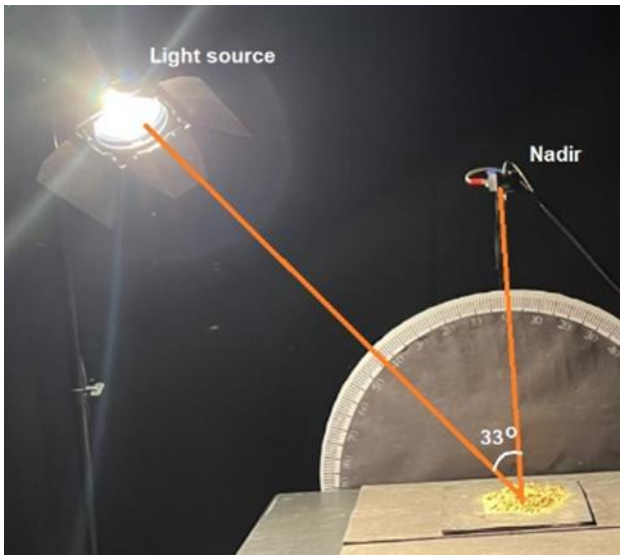

Figure 2. Light source and its zenith angle configuration.

For each material, radiance measurements were carried out in intervals of 10 degrees from nadir in the forward and backward directions, from (-70) to 70 degrees. Each sample included a measurement of the target's radiance acquired by the spectroradiometer and an RGB image of the scene.

3.3 Target objects/materials

We used three abundant materials as targets: dry dark clumpy soil, slightly clumpy yellow soil, and glossy leaves. The surface texture and microtopography are the main factors for BRDF differences between various surfaces. Thus, the targets were chosen accordingly from very clumpy soil with highly asymmetrical soil clumps, soil with nearly symmetrical, almost elliptical smooth clumps, and smooth glossy broad leaves of *Arum palaestinum*.

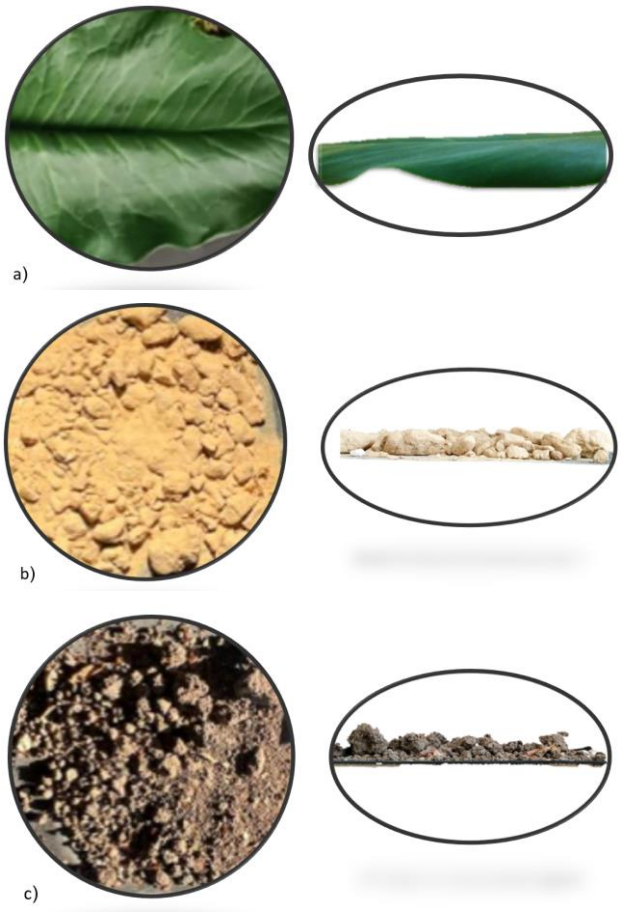

Figure 3. Target objects in a top view (left column) and a side view (right column): a) glossy leaves of Arum palaestinum; b) bright soil with nearly symmetrical, almost elliptical smooth clumps; c). dark soil with asymmetric clumps

4. RESULTS AND DISCUSSION

The nature of the reflection depends on the surface irregularities, such as roughness or smoothness, relative to the wavelength of the considered radiation (Shoshany, 1993). For example, the is smoother is a surface, the more specular reflection occurs. On the other hand, as the surface is rough, it will act as a diffuse. To evaluate the accuracy of the proposed methodology for BRDF measurements, we first examined the estimated sensor location. Then we observed the BRDF of the three selected materials.

4.1 Extraction of sensor location and comparison between retrieved from SFM algorithm and measured by protractor

We first feed the SFM process with the RGB images of observed scenes at all zenith angles (fifteen images in our case). Figure 4 presents nine out of the fifteen images acquired to retrieve the sensor locations in the dark soil BRDF scene. Texture patterns were distributed around the sample to enhance the image feature extraction. These images are the only input for the SFM.

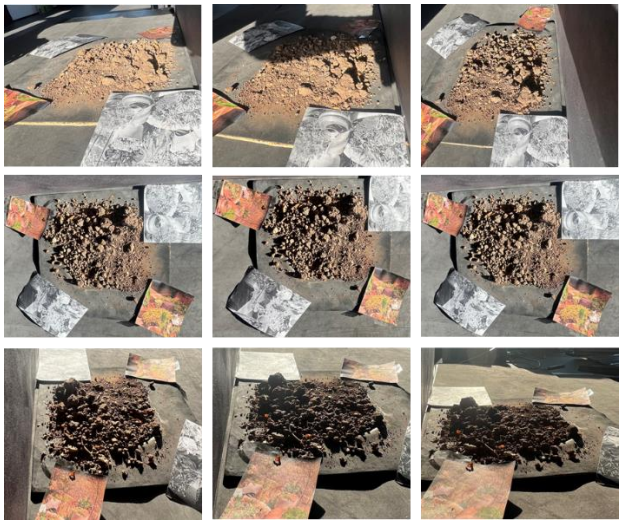

Figure 4. Nine of the fifteen acquired images for the BRDF scene of dark soil.

Figure 5 presents the scene's 3D model and camera locations obtained using the SFM are in an arbitrary coordinate system.

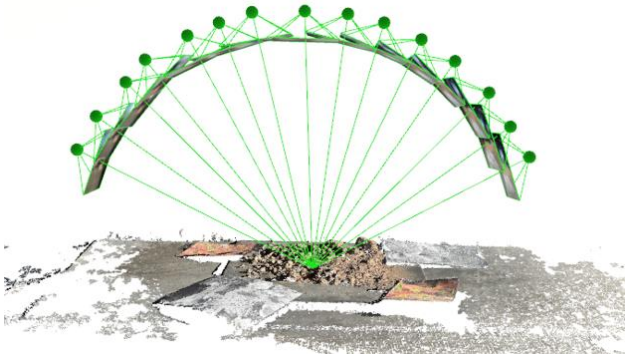

Figure 5. Automatically derived scene's 3D model and sensor's location for a set of images using SFM.

Once we obtained the SFM outputs, we computed the sensor's zenith angle and its distance from the scene's center in each measurement, as presented in section 2.2 (see Table 1).

Image	Measured (GT) (degrees)	Estimated (degrees)	Difference (degrees)
1	-70.00	-68.90	1.10
2	-60.00	-59.68	0.32
3	-50.00	-48.91	1.09
4	-40.00	-41.49	1.49
5	-30.00	-29.69	0.31
6	-20.00	-21.39	1.39
7	-10.00	-11.00	1.00
8	0.00	0.00	0.00
9	10.00	10.75	0.75
10	20.00	20.01	0.01
11	30.00	30.21	0.21
12	40.00	40.16	0.16
13	50.00	51.29	1.29
14	60.00	61.11	1.11
15	70.00	70.01	0.01
			Mean = 0.68
			Max= 1.49

Table 1: Comparison between the angles measured by protractor and retrieved by SFM algorithm using RGB images.

In addition, we converted the distance from arbitrary units into centimeters by setting the distance of the vertical image to 65cm as measured in the auxiliary device (see Table 2).

Image	Measured (GT) (Centimeters)	Estimated (Centimeters)	Difference (Centimeters)
1	65.00	71.15	6.15
2	65.00	69.95	4.95
3	65.00	68.53	3.53
4	65.00	68.62	3.62
5	65.00	66.82	1.82
6	65.00	66.15	1.15
7	65.00	66.13	1.13
8	65.00	65.00	0.00
9	65.00	65.44	0.44
10	65.00	65.91	0.91
11	65.00	66.37	1.37
12	65.00	67.03	2.03
13	65.00	67.61	2.61
14	65.00	67.49	2.49
15	65.00	69.51	4.51
			Mean = 2.45
			Max= 6.15

Table 2: Estimated distance from each image to the scene center as derived using the SFM outputs.

4.2 Results of BRDF measurements using a camera-aided spectroradiometer

Figure 6 presents the reflectance spectra for the three examined natural surfaces measured from different observation zenith angles.

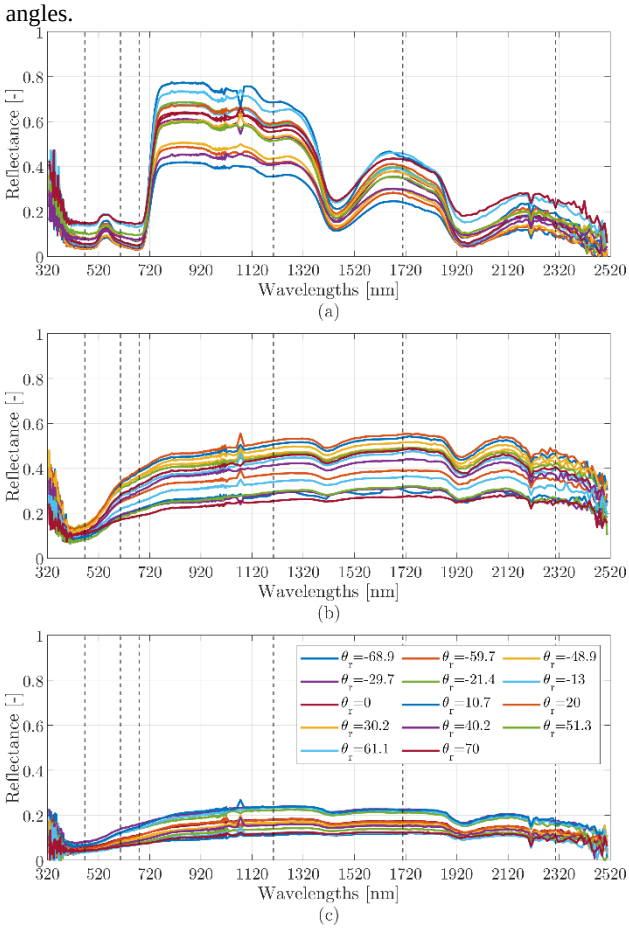

Figure 6. Reflectance spectra variations at various viewing zenith angles for a) glossy leaves, b) bright soil and c) dark soil.

The vertical dashed lines indicate six spectral bands that we use to understand the BRDF characteristics further.

The results clearly show the variability in the spectra that occurred due to the BRDF effect. However, they provide only a general sense of the difference between the measurements from the different directions. Thus, to further understand the surfaces' BRDF characteristics, we select six spectral bands and observe the reflectance vs. the viewing zenith angle. Figure 7 presents the results for the three bands in the Vis-NIR area, and Figure 8 presents the three in the SWIR area.

The sensor, the light source, and the target were always in the same plane (the so-called principle plane). Thus, we set the azimuth to the left and right sides relative to the vertical direction to 0 and 180, respectively. Accordingly, we defined negative and positive zenith angles corresponding to sensor location with an azimuth value of 0 and 180, respectively. In the BRDF scenario, the measurements from the side of the light source (i.e., with an azimuth of 0 degrees and negative zenith angle in our case) capture the backward scattering from the surface, whereas the measurements from the other side capture the forward scattering.

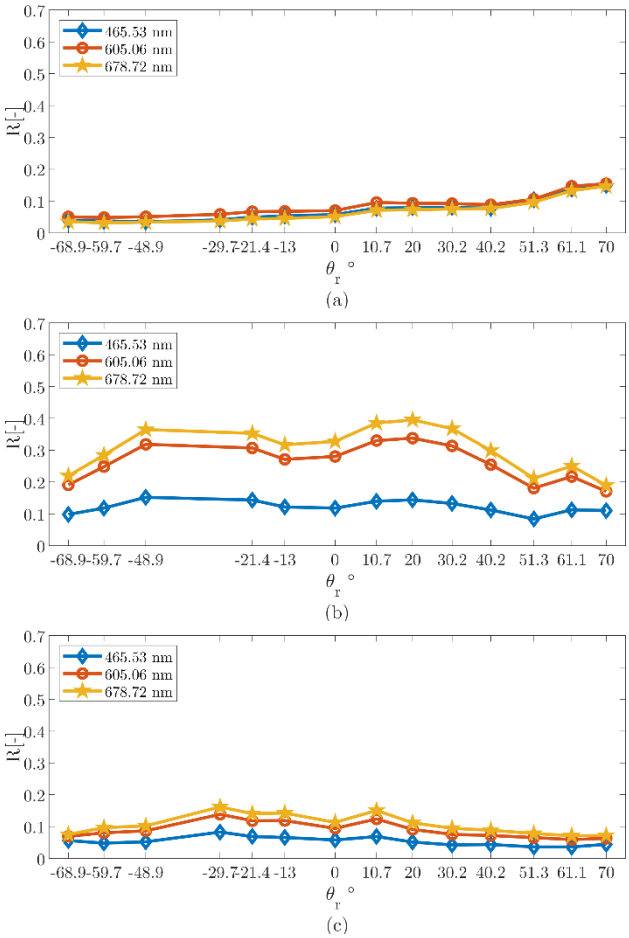

Figure 7. Bidirectional reflectance vs. the observation zenith angles, retrieved by SFM, in three spectral bands in the Vis-NIR range, 465.53 nm, 605.06 nm, and 678.72 nm from a) glossy leaves, b) bright soil, and c) dark soil.

The results in both the Vis-NIR and SWIR regions show that a BRDF with a nearl-diffuse scattering characterizes both soil types. On the other hand, the forward scattering from vegetation leaf (*Arum palaestinum*) is significantly higher than the backword scattering, indicating a near gloss surface, as expected.

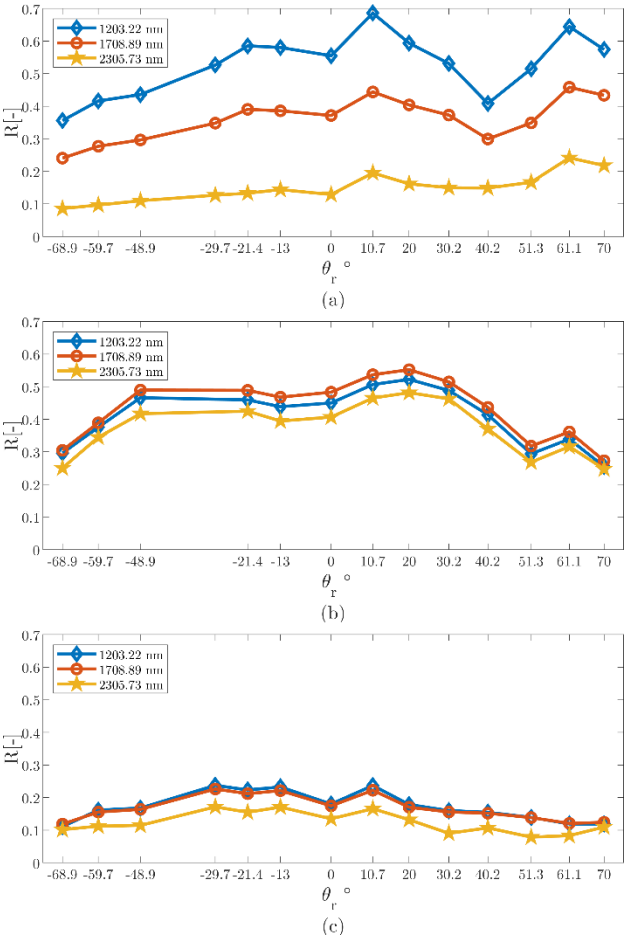

Figure 8. Bidirectional reflectance vs. the observation zenith angles, retrieved by SFM, in three spectral bands in the SWIR range: 1203.22 nm, 1708.89 nm, and 2305.73 nm, from a) glossy leaves, b) bright soil, and c) dark soil.

The reflectance spectra in Figure 6 show that all measurements of a particular material are correlated. The shape of the obtained spectral signatures from the different viewing zenith angles is similar but with different magnitudes. To test the variability of the measured reflectance, we compute the Coefficient of Variation (CV) for each spectral band. The CV is computed by the standard deviation of the fifteen spectral measurements (from the different viewing angles) divided by their mean value.

Figure 10 presents the three tested materials' CV values per spectral band. The results show a high noise rate at the periphery of the spectral ranges: under 400nm and above 2400nm. Otherwise, the CV values for the two soil types are closely constant, i.e., the normalized variability between the measurements is similar in the different spectral bands. On the other hand, the CV in measurement for the glossy leaf increases significantly in the bands around 450nm, 600nm, and 1950nm.

Finally, to examine the error in retrieving the zenith angles through SFM and its influence on the BRDF measurement, we compared the results to the GT values measured by the protractor. Figure 10 presents the measure reflectance vs. the measured (GT) and retrieved zenith angle values. The plots show that retrieved values are almost identical to the measured ones. Accordingly, there is only a minor and meaningless shift in the BRDF signal, indicating the high accuracy of the proposed methodology in measuring the BRDF of material surfaces.

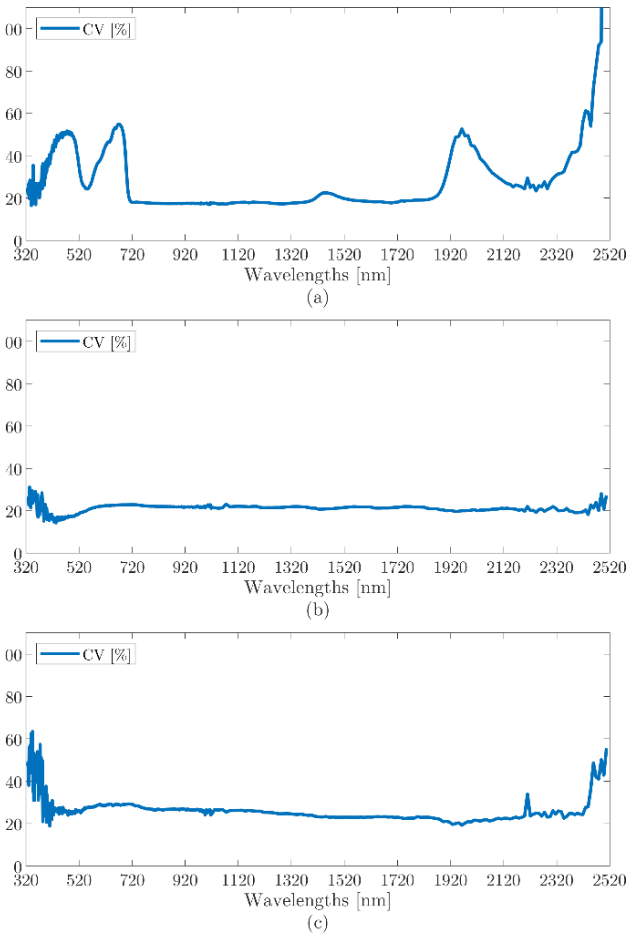

Figure 9. The CV values in different spectral bands for a) glossy leaves, b) bright soil, and c) dark soil.

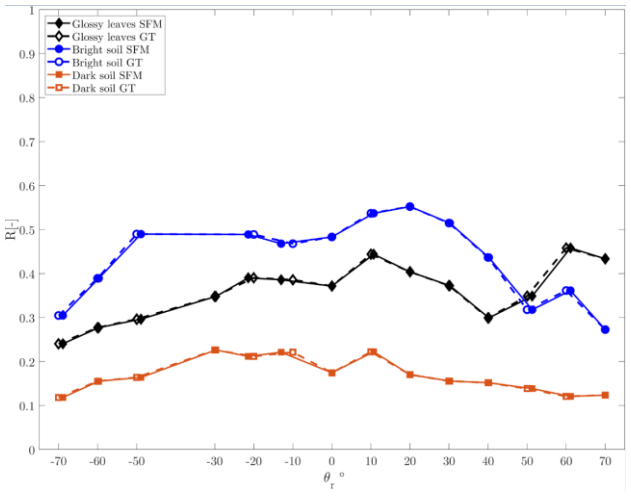

Figure 10. Bidirectional reflectance as a function of retrieved by SFM and measured by protractor zenith observation angles in the spectral band of 1708.89 nm for three target materials.

Besides, according to Figure 10., the glossy leaves have two reflection hot spots in the forward direction, around $\theta_r = 10°$ and at $\theta_r = 60°$. While the dark soil with asymmetric clumps reflects more light in the backward than in the forward direction. The light soil with symmetric clumps reflects almost equally in both directions, but mainly in the forward direction.

5. CONCLUSIONS

We studied the BRDF measurement using a camera-aided spectrometer and proposed a new methodology for retrieving the sensor location in the BRDF scenario without unique equipment.

To evaluate the performance of the proposed methodology, we measured the BRDF of three surfaces with different roughness. The comparison to ground truth measurements revealed that the sensor locations retrieved by the SFM are almost identical to those measured by an auxiliary device. Accordingly, the results clearly show that the camera-aided spectroradiometer allows measuring the BRDF with very high accuracy. Currently, we successfully implemented measurements of radiance using a camera-aided spectroradiometer in the laboratory and intend to examine its potential for BRDF measurements in future work. For example, further research will be dedicated to the BRDF experiments using a camera-aided spectroradiometer with no auxiliary devices. The researcher will freely hold the spectroradiometer and point toward the observed scene. The spectroradiometer probe was connected to a rigid arm; thus, the distance between the observed object and the probe remained constant. However, in the second stage, distance correction should be considered. The radiance obtained from the surface is inversely related to the square distance between the probe and surface. Besides, we will examine outdoor measurements under natural conditions and the sun as a light source.

REFERENCES

Lanevski, D., Manoocheri, F., Ikonen, E., 2022. Gonioreflectometer for measuring 3D spectral BRDF of horizontally aligned samples with traceability to SI. Metrologia, 59(2), 025006

Li, H., Foo, S-C, Torrance, K. E., Westin, S. H., 2006. Automated three-axis gonioreflectometer for computer graphics applications. Opt. Eng. 45 043605

Martonchik, J. V., Bruegge, C.J., Strahler, A.H., 2000. A review of reflectance nomenclature used in remote sensing. Remote Sens. Rev. 19, 9–20. DOI:10.1080/02757250009532407

Nicodemus, F., Richmond, J., Hsia, J., 1977. Geometrical considerations and nomenclature for reflectance. Sci. Technol. 60, 1–52. DOI:10.1109/LPT.2009.2020494

Özyeşil, O., Voroninski, V., Basri, R., Singer¸ A., 2017. A survey of structure from motion. Acta Numer. 26, 305–364. DOI:10.1017/S096249291700006X

Spectral Evolution RS-8800 Remote Sensing Bundle, https://spectralevolution.com/products/hardware/field-portable-spectroradiometers-for-remote-sensing/rs-8800-remote-sensing-bundle/

Shoshany M., 1993. Roughness-Reflectance Relationship of Bare Desert Terrain: an Empirical Study. Remote Sens. Environ. 45:15-27

Silva, L. F., 1978. Radiation and Instrumentation in Remote Sensing. In: Remote sensing : The quantitative approach, edited by Swain P.H., Davis, S.M.. New York : McGraw-Hill

Spectra Vista Corporation, https://spectravista.com/

White D.R. et al., 1998. Reflectometer for Measuring the Bidirectional Reflectance of Rough Surface, Applied Optics 37:16.